Thermal convection and radiation in a rotating cabinet with time-dependent heat-generated solid element and heat-conducting solid walls

Received 2 October 2020
Revised 30 December 2020
Accepted 3 January 2021

Stepan Mikhailenko
Laboratory on Convective Heat and Mass Transfer, National Research Tomsk State University, Tomsk, Russian Federation

Mohammad Ghalambaz
Faculty of Applied Sciences, Ton Duc Thang University, Ho Chi Minh City, Vietnam, and

Mikhail A. Sheremet
Laboratory on Convective Heat and Mass Transfer, National Research Tomsk State University, Tomsk, Russian Federation

Abstract

Purpose – This paper aims to study numerically the simulation of convective–radiative heat transfer under an effect of variable thermally generating source in a rotating square chamber. The performed analysis deals with a development of passive cooling system for the electronic devices.

Design/methodology/approach – The domain of interest of size H rotating at a fixed angular velocity has heat-conducting solid walls with a constant cooling temperature for the outer boundaries of the vertical walls and with thermal insulation for the outer borders of the horizontal walls. The chamber has a heater on the bottom wall with a time-dependent volumetric heat generation. The internal surfaces of the walls and the energy element are both grey diffusive emitters and reflectors. The fluid is transparent to radiation. Computational model has been written using non-dimensional parameters and worked out by the finite difference technique. The effect of the angular velocity, volumetric heat generation frequency and surface emissivity has been studied and described in detail.

Findings – The results show that growth of the surface emissivity leads to a diminution of the mean heater temperature, while a weak rotation can improve the energy transport for low volumetric thermal generation frequency.

Originality/value – An efficient computational approach has been used to work out this problem. The originality of this work is to analyze complex (conductive–convective–radiative) energy transport in a rotating system with a local element of time-dependent volumetric heat generation. To the best of the authors' knowledge, an interaction of major heat transfer mechanisms in a rotating system with a heat-generating element is scrutinized for the first time. The results would benefit scientists and engineers to become familiar with the analysis of complex heat transfer in rotating enclosures with internal heat-generating units, and the

This work was supported by the Russian Science Foundation (Project No. 17–79-20141). The authors also wish to thank the very competent reviewers for the valuable comments and suggestions.

International Journal of Numerical Methods for Heat & Fluid Flow
Vol. 31 No. 12, 2021
pp. 3527-3546

0961-5539
DOI 10.1108/HFF-10-2020-0614

way to predict the heat transfer rate in advanced technical systems, in industrial sectors including transportation, power generation, chemical sectors and electronics.

Keywords Natural convection, Cooling, Radiative heat transfer, Heat-conducting solid walls, Rotating cavity, Variable heat generation

Paper type Research paper

Nomenclature

Roman letters

c = thermal capacity, (J·kg^{-1}·K^{-1});
f = non-dimensional volumetric thermal generation frequency;
$F_{k\text{-}i}$ = view factor from kth portion to the ith portion of the chamber;
g = gravity acceleration, (m·s^{-2});
H = length of the chamber, (m);
J_k = radiosity for the kth portion, (W·m^{-2})ss;
l = thickness of the solid walls, (m);
N_{rad} = radiation number;
$\overline{Nu}_{conv}$ = mean convective Nusselt number;
$\overline{Nu}_{rad}$ = mean radiation Nusselt number;
NS = quantity of surface portions in the chamber;
p = pressure, (Pa);
Pr = Prandtl number;
q_k = irradiance for the kth portion, (W·m^{-2});
q_{rad} = radiation thermal flux, (W·m^{-2});
Q_{vol} = volumetric thermal flux, (W·m^{-3});
Q = time-dependent volumetric thermal flux, (W·m^{-3});
Q_{rad} = non-dimensional net radiation thermal flux;
Ra = Rayleigh number;
R_k = non-dimensional radiosity of the kth portion of the chamber;
t = time, (s);
T = temperature, (K);
T_c = cold border temperature, (K);
Ta = Taylor number;
$\overline{u}, \overline{v}$ = velocity components, (m·s^{-1});
u, v = non-dimensional velocity components;
$\overline{x}, \overline{y}$ = coordinates, (m); and
x, y = non-dimensional coordinates;

Greek symbols

α = heat diffusivity, (m^2·s^{-1});
β = heat expansion parameter, (K^{-1});
γ = temperature parameter;
ΔT = temperature difference, (K);
ε = surface emissivity;
ζ = dimensional volumetric heat generation frequency, (s^{-1});
θ = non-dimensional temperature;
λ = heat conductivity, (W·m^{-1}·K^{-1});
μ = dynamic viscosity, (Pa·s);
ν = kinematic viscosity, (m^2·s^{-1});

ξ_0 = angular velocity, (s^{-1});
ρ = fluid density, ($kg \cdot m^{-3}$);
σ = Stefan-Boltzmann parameter, ($W \cdot m^{-2} \cdot K^{-4}$);
τ = non-dimensional time;
ϕ = angle of rotation;
$\overline{\psi}$ = stream function, ($m^2 \cdot s^{-1}$);
ψ = non-dimensional stream function;
$\overline{\omega}$ = vorticity, (s^{-1}); and
ω = non-dimensional vorticity;

Subscripts

avg = average value;
c = cold wall;
conv = convective mechanism;
f = fluid;
hs = heat source;
max = maximum value;
rad = radiative mechanism; and
w = wall;

1. Introduction

The problem of convective energy transfer is very common today and it is an integral part of various production and natural processes. A very interesting area is the task on cooling of the electronic equipment. The equipment is heated because of the electric currents passing in it during operations; therefore, proper cooling is required for correct and long-term exploitation. Often systems with electronics are involved in rotational motion, for example, in the space industry (Banerjee *et al.*, 2009), in crystal growth (Fedyushkin, 2019; Nguyen *et al.*, 2019) and in many other fields. Studies on convective–radiative heat transfer are well suited to solve such problems (Bahlaoui *et al.*, 2006; Sivaraj and Sheremet, 2018; Kogawa *et al.*, 2019).

So, interaction of thermal radiation and convective energy transport in a square chamber under an influence of separate cylindrical elements has been investigated by Boukendil *et al.* (2020). The convective motion in the cavity has been driven by partially heating cylinder and asymmetrically cooled walls. The obtained results show a significant impact of the heat radiation on the energy transport. Thermal convection and radiation in the square chamber has been examined by Ayachi *et al.* (2012). The cavity has been deferentially heated and cooled by two configurations, namely, vertical-bottom and vertical-top heated elements. System of the control partial differential equations has been approximated by the finite difference technique and worked out by over-relaxation and alternate direction implicit methods. Results have shown that vertical-bottom heating assists to enhance the flow circulations and increase in the Nusselt number, while vertical-top configuration slows the liquid motion and energy transference. Billaud *et al.* (2017) have examined complex energy transport in differentially heated cubic cavity. The cavity has been filled with a sensitive to radiation dry air with water vapor. The boundary layer thickness, heat stratification characteristic and three-dimensional features have been compared with pure air convection regime. Authors found that global circulation and heat transfer strongly depend on the cavity length. The influence of heat radiation on magneto-convective transport of electrically conducting medium has been examined by Jena and Mahapatra (2014). Three-dimensional control equations have been discretized using the control volume technique.

Results have shown a reduction of convective energy transference strength with surface emissivity in the case of low magnetic influence, whereas in the case of great magnetic influence, convective energy transference strength rises with a growth of surface emissivity. Ridouane *et al.* (2004) have scrutinized the convective–radiative energy transmission in the differentially warmed chamber. The cavity has insulated vertical boundaries, warmed lower boundaries and cooled upper boundaries. The authors have observed a weak impact of surface emissivity on convective *Nu*, while total *Nu*, as well as radiation Nusselt number, grow monotonically with surface emissivity.

Periodically heated solid blocks are well suited for modeling the non-permanent heating of an element of electronic equipment. For example, thermal and mass transmission driven by mixed convective transport and pulsating heated electronic component has been researched by Ghasemi (2005). Results have shown that the mean *Nu* and high temperature heavily depend on heating frequency and a rising of *Ra* reflects in energy transference enhancement. Huang *et al.* (2014) have studied regimes of thermal convective transport in a cubic chamber having varying heated sidewall. The authors have claimed that the energy transmission augmentation is significantly dependent on *Ra*, sidewall pulsating period and amplitude. The resonance of natural convection has been found for high *Ra* and sidewall temperature pulsating period. Other interesting results on periodic heating can be found in Alsabery *et al.* (2017), Sheremet *et al.* (2018), Oosthuizen (1999), Alsabery *et al.* (2016) and Alsabery *et al.* (2019).

Using the heat-conducting solid walls makes the studies more detailed, which allows a more accurate exploration of the temperature distribution (Zhang *et al.*, 2012; Nouanegue *et al.*, 2009; Zargartalebi *et al.*, 2017; Miroshnichenko *et al.*, 2016). For example, Zhang *et al.* (2012) have investigated thermal convective transport in a tilted cubic chamber with solid walls. The system of dimensionless control equations has been solved by high-accuracy multidomain pseudospectral method. It has been found that a presence of walls reflects in diminishing of temperature gradient across the cavity. Thermal convective and radiative transport in a tilted square region having solid wall has been performed by Nouanegue *et al.* (2009). The solid wall has a fixed temperature, while the opposite border has a fixed thermal flux. Authors have found that interaction of convection, radiation and conduction is strong. The impact of thermal radiation on convective transport is non-negligible and it can essentially modify the thermal and velocity patterns. Other useful results on complex natural convection can be found in Zargartalebi *et al.* (2017), Miroshnichenko *et al.* (2016), Sen and Sarkar (1995), Saravanan and Sivaraj (2017) and Abdollahzadeh Jamalabadi *et al.* (2013).

More tasks affecting the topics described above can be found in El Ayachi *et al.* (2008), Xin *et al.* (2013), Wang *et al.* (2011) and Zhang *et al.* (2011). For example, convective–radiative energy transport in differentially heated square cavity with periodic temperature has been described by El Ayachi *et al.* (2008). The left vertical boundary of the chamber was warmed sinusoidal with time, while right border was kept at fixed temperature. Authors have claimed that a proper choice of the parameters can significantly enhance the energy transfer strength compared to the mode of constant warming. Xin *et al.* (2013) have solved the problem of stratification discrepancy of turbulent convective transport in differentially warmed chambers. An improvement in the numerical experiment has been achieved using improved data metrology, the addition of obtained experimentally temperature profiles on passive boundaries and also taking into account heat radiation. Nice agreement between theoretical and experimental data has been achieved. The interaction of energy transport mechanisms in open chamber under an impact of constant heat flux has been examined computationally by Wang *et al.* (2011). The governing equations have been worked out using simple method and quick approach. The data have shown that solid wall conduction

and heat radiation increase the total *Nu*. The heat convective transport inside a tilted enclosure with solid walls under an effect of time-periodic warming has been carried out by Zhang *et al.* (2011). The high-accuracy multidomain temporal-spatial pseudospectral method has been used for an investigation of the problem. It has been ascertained that total energy transport linearly rises with thermal conductivity and diffusivity ratio and depends on pulsating sidewall temperature. Thermal transference rate rises with a growth of pulsating amplitude and diminishes with an inclination angle.

Also problems involving rotating systems are very interesting and useful for different engineering applications. Rotating cooling can be applied in electric motors, solar power systems, space industry, crystal growth and others. For example, Wu *et al.* (2014) have scrutinized the impact of rotation on convective transport in a rotating chamber for solar receiver. Authors have suggested a new concept for high-temperature solar receiver. Results have shown that thermal losses because of rotation can be less than 1%. Jin *et al.* (2005) have scrutinized computationally and experimentally the convective transport in a rotating chamber under an effect of discrete heat sources. The cavity includes heater covered by Teflon and Lexan walls. Authors have shown non-stationary velocity and temperature patterns in the liquid part and stable temperature field in solid zone. The influence of rotation on energy transport in solid areas is weak. Convection in a rotating cubical region warmed from bottom surface has been examined by Sedelnikov *et al.* (2012). The obtained data have been presented for moderate Rayleigh numbers, Coriolis parameters and Prandtl numbers. The results have shown different flow patterns when the Rayleigh number changes. Authors have determined the critical *Ra* for the onset of convective transport. The convective heat transfer and entropy generation in a wavy porous cavity with rotating cylinder has been investigated by Alsabery *et al.* (2018). It has been shown that the highest values of the average Nusselt number are achieved at high values of the Darcy number and low values of the rotation rate. Therefore, rotation does not always lead to improved heat transfer. The influence of the inclination angle of the studied areas on heat and mass transfer may also be of interest. Transient natural convection in a nanofluid porous inclined cavity has been studied using local thermal non-equilibrium approach model by Sivasankaran *et al.* (2018). The paper has shown how the cavity inclination angle can change the flow patterns.

The presented brief review of the papers shows modern state of the art of convective energy transport under the impact of surface radiation, heat-conducting solid walls and local heaters. It is worth noting that rotating chamber with variable heating elements under the influence of three types of energy transference (convection, conduction and radiation) has not been previously studied. Therefore, this study is aimed at numerical modeling of convective–radiative energy transport inside a square rotating chamber with a non-uniform heating element and solid heat-conducting walls. This research can be applied to the development of passive cooling systems for electronic devices in various engineering applications including heat exchangers, solar collectors, chemical reactors and others.

2. Basic equations

Thermal convective transport combined with surface radiation in a closed chamber of size H rotating at a fixed angular velocity ξ_0 shown in Figure 1 has been scrutinized numerically. The chamber has heat-conducting walls of width $l = H/12$ (walls width equals 10% of interior camera) and a heater on the bottom wall with variable volumetric heat generation $Q = 0.5Q_{vol}\{1 - \sin(\zeta \pi t)\}$. The external surfaces of the horizontal walls are adiabatic, while the external boundaries of the others are kept at a fixed cooling temperature T_c. The chamber is filled with a fluid satisfying the Boussinesq approximation. Fluid of $Pr = 0.7$ (air) is Newtonian and incompressible and all physical parameters are not dependent on

temperature, except for the density mentioned above. The physical parameters of the bottom wall correspond to the textolite, the remaining walls correspond to aluminum and the heat source material is silicon. The internal surfaces of the walls and the energy element are both gray diffusive emitters and reflectors. The fluid is transparent to radiation. The fluid motion and energy transport are two-dimensional and laminar.

Given all the assumptions, the system of equations describing complex energy transference in a rotating region having a thermally generating element follows as (Mikhailenko *et al.*, 2018; Mikhailenko and Sheremet, 2020; Mikhailenko *et al.*, 2020):

- for the liquid region:

$$\frac{\partial \overline{u}}{\partial \overline{x}} + \frac{\partial \overline{v}}{\partial \overline{y}} = 0 \tag{1}$$

$$\rho\left(\frac{\partial \overline{u}}{\partial t} + \overline{u}\frac{\partial \overline{u}}{\partial \overline{x}} + \overline{v}\frac{\partial \overline{u}}{\partial \overline{y}}\right) = -\frac{\partial p}{\partial \overline{x}} + \mu\left(\frac{\partial^2 \overline{u}}{\partial \overline{x}^2} + \frac{\partial^2 \overline{u}}{\partial \overline{y}^2}\right) + \\ + \rho g \beta (T - T_c)\sin(\xi_0 t) - \rho \beta (T - T_c)\xi_0^2 \overline{x} + 2\rho \overline{v}\,\xi_0 \tag{2}$$

$$\rho\left(\frac{\partial \overline{v}}{\partial t} + \overline{u}\frac{\partial \overline{v}}{\partial \overline{x}} + \overline{v}\frac{\partial \overline{v}}{\partial \overline{y}}\right) = -\frac{\partial p}{\partial \overline{y}} + \mu\left(\frac{\partial^2 \overline{v}}{\partial \overline{x}^2} + \frac{\partial^2 \overline{v}}{\partial \overline{y}^2}\right) + \\ + \rho g \beta (T - T_c)\cos(\xi_0 t) - \rho \beta (T - T_c)\xi_0^2 \overline{y} - 2\rho \overline{u}\,\xi_0 \tag{3}$$

$$\frac{\partial T}{\partial t} + \overline{u}\frac{\partial T}{\partial \overline{x}} + \overline{v}\frac{\partial T}{\partial \overline{y}} = \frac{\lambda_f}{(\rho c)_f}\left(\frac{\partial^2 T}{\partial \overline{x}^2} + \frac{\partial^2 T}{\partial \overline{y}^2}\right) \tag{4}$$

- for the heat source:

$$\rho_{hs} c_{hs}\frac{\partial T}{\partial t} = \lambda_{hs}\left(\frac{\partial^2 T}{\partial \overline{x}^2} + \frac{\partial^2 T}{\partial \overline{y}^2}\right) + Q \tag{5}$$

- for the solid walls:

$$\rho_w c_w \frac{\partial T}{\partial t} = \lambda_w\left(\frac{\partial^2 T}{\partial \overline{x}^2} + \frac{\partial^2 T}{\partial \overline{y}^2}\right) \tag{6}$$

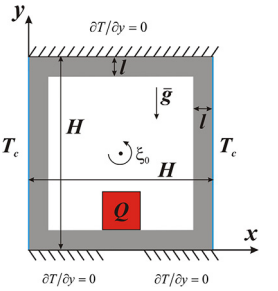

Figure 1.
Physical model

The no-slip boundary condition is applied for velocity vector on the internal walls of the chamber and on the heater surface. Thermal boundary conditions are:

- at the external walls surface $\overline{x} = 0$ and $\overline{x} = H$ temperature is fixed: $T = T_c$;
- at the external walls surface $\overline{y} = 0$ and $\overline{y} = H$ an adiabatic condition is used: $\frac{\partial T}{\partial \overline{y}} = 0$;
- at the heat source surfaces: $\begin{cases} T_f = T_{hs} \\ -\lambda_f \dfrac{\partial T_f}{\partial n} + q_{\text{rad}} = -\lambda_{hs} \dfrac{\partial T_{hs}}{\partial n} \end{cases}$
- at the internal solid walls surfaces: $\begin{cases} T_f = T_w \\ -\lambda_f \dfrac{\partial T_f}{\partial n} + q_{\text{rad}} = -\lambda_w \dfrac{\partial T_w}{\partial n} \end{cases}$

The radiative heat flux from the wall section q_{rad} can be described as the difference between the outgoing heat radiation (radiosity) and incoming heat radiation (irradiance). Using the net radiation technique (Mikhailenko *et al.*, 2018; Mikhailenko and Sheremet, 2020; Mikhailenko *et al.*, 2020), the resulting thermal radiative flux for the k-th differential element is formulated as $q_{\text{rad},k} = J_k - q_k$, where J_k is the radiosity for the k-th differential element and $q_k = \sum_{i=1}^{NS} F_{k-i} J_i$ is the irradiance for the k-th differential element.

The radiosity for a diffusive opaque surface is assumed of emitted plus reflected energy like: $J_k = \varepsilon_k \sigma T_k^4 + (1 - \varepsilon_k) q_k$ or

$$J_k = \varepsilon_k \sigma T_k^4 + (1 - \varepsilon_k) \sum_{i=1}^{NS} F_{k-i} J_i \tag{7}$$

where NS is the total number of surface segments composing the solid–fluid interface and the heat source, F_{k-i} is a view factor and ε_k is the emissivity of the k-th differential element.

Setting special functions defined as vorticity $\left(\overline{\omega} = \frac{\partial \overline{v}}{\partial \overline{x}} - \frac{\partial \overline{u}}{\partial \overline{y}}\right)$ and stream function $\left(\overline{u} = \frac{\partial \overline{\psi}}{\partial \overline{y}}, \overline{v} = -\frac{\partial \overline{\psi}}{\partial \overline{x}}\right)$ and using dimensionless parameters:

$$x = \overline{x}/H, \quad y = \overline{y}/H, \quad \tau = \xi_0 t, \quad u = \overline{u}/(\xi_0 H), \quad v = \overline{v}/(\xi_0 H),$$
$$\psi = \overline{\psi}/\left(\xi_0 H^2\right), \quad \omega = \overline{\omega}/\xi_0, \quad \theta = (T - T_c)/\Delta T, \quad \Delta T = Q_{vol} H^2/\lambda_{hs}, \quad f = \zeta/\xi_0 \tag{8}$$

The system of the control equations (1)–(6) is formulated in non-dimensional form:

- for the liquid zone:

$$\frac{\partial^2 \psi}{\partial x^2} + \frac{\partial^2 \psi}{\partial y^2} = -\omega \tag{9}$$

$$\frac{\partial \omega}{\partial \tau} + u \frac{\partial \omega}{\partial x} + v \frac{\partial \omega}{\partial y} = \frac{1}{\sqrt{Ta}} \left(\frac{\partial^2 \omega}{\partial x^2} + \frac{\partial^2 \omega}{\partial y^2} \right) + \frac{Ra}{Pr \cdot Ta} \left[\frac{\partial \theta}{\partial x} \cos(\tau) - \frac{\partial \theta}{\partial y} \sin(\tau) \right] \tag{10}$$

$$\frac{\partial \theta}{\partial \tau} + u\frac{\partial \theta}{\partial x} + v\frac{\partial \theta}{\partial y} = \frac{1}{Pr\sqrt{Ta}}\left(\frac{\partial^2 \theta}{\partial x^2} + \frac{\partial^2 \theta}{\partial y^2}\right) \tag{11}$$

- for the solid block:

$$\frac{\partial \theta}{\partial \tau} = \frac{\alpha_{hs}/\alpha_f}{\sqrt{Ra \cdot Pr}}\left(\frac{\partial^2 \theta}{\partial x^2} + \frac{\partial^2 \theta}{\partial y^2} + \frac{1}{2}\{1 - \sin(f\pi\tau)\}\right) \tag{12}$$

- for the solid walls:

$$\frac{\partial \theta}{\partial \tau} = \frac{\alpha_w/\alpha_f}{\sqrt{Ra \cdot Pr}}\left(\frac{\partial^2 \theta}{\partial x^2} + \frac{\partial^2 \theta}{\partial y^2}\right) \tag{13}$$

where $\mathrm{Ra} = g\beta\Delta T H^3/(\alpha\nu)$ is the Rayleigh number; $Pr = \nu/\alpha$ is the Prandtl number; and $Ta = {\xi_0}^2 H^4/\nu^2$ is the Taylor number.

The initial and boundary conditions are:

- $\tau = 0: \quad \psi = \omega = \theta = 0 \ \text{at}\, 0 \le x \le 1 \,\text{and}\, 0 \le y \le 1$ (14a)

$\theta = 0 \ \text{at}\, x = 0, 1 \,\text{and}\, 0 \le y \le 1;$

- $\dfrac{\partial \theta}{\partial y} = 0 \ \text{at}\, y = 0, 1 \,\text{and}\, 0 < x < 1$ (14b)

- at the thermally generating element surface:

$$\psi = 0,\ \omega = -\frac{\partial^2 \psi}{\partial n^2},\ \begin{cases} \theta_{hs} = \theta_f \\ \dfrac{\lambda_{hs}}{\lambda_f}\dfrac{\partial \theta_{hs}}{\partial n} = \dfrac{\partial \theta_f}{\partial n} - N_{\mathrm{rad}} Q_{\mathrm{rad}} \end{cases} \tag{14c}$$

- at the internal walls surfaces:

$$\psi = 0,\ \omega = -\frac{\partial^2 \psi}{\partial n^2},\ \begin{cases} \theta_w = \theta_f \\ \dfrac{\lambda_w}{\lambda_f}\dfrac{\partial \theta_w}{\partial n} = \dfrac{\partial \theta_f}{\partial n} - N_{\mathrm{rad}} Q_{\mathrm{rad}} \end{cases} \tag{14d}$$

Here $N_{rad} = \sigma T_c^4 H/(\lambda\Delta T)$ is a radiation number.

The dimensionless net radiative heat flux is defined as follows:

$$Q_{rad,k} = R_k - \sum_{i=1}^{NS} F_{k-i} R_i \tag{15}$$

and dimensionless radiosity:

$$R_k = (1 - \varepsilon_k)\sum_{i=1}^{NS} F_{k-i} R_i + \varepsilon_k (1 - \gamma)^4 \left(\theta_k + 0.5\frac{\gamma}{1 - \gamma}\right)^4 \tag{16}$$

Mean convective and radiative Nusselt numbers at heat-generating element surface have been chosen for analysis of the heat transfer rate and written as:

$$\overline{Nu}_{conv} = -\frac{1}{l}\int_0^l \frac{\partial\theta}{\partial n} d\zeta, \quad \overline{Nu}_{rad} = -\frac{N_{\text{rad}}}{l}\int_0^l Q_{\text{rad}} d\zeta \tag{17}$$

Here ζ is the heat-generating element surface.

3. Computational technique and validation

The set of the control equations of complex energy transference in a rotating chamber having solid walls under an effect of variable heat-generating block [equations (9)–(13)] with initial and boundary conditions [equation (14)] has been studied numerically (Sheremet *et al.*, 2018; Miroshnichenko *et al.*, 2016; Mikhailenko *et al.*, 2018; Mikhailenko *et al.*, 2020). Calculations have been performed using the uniform grid by the finite difference technique. The stream function equation has been discretized by central differences. The successive over-relaxation algorithm has been used for solving the obtained linear discretized equations. The vorticity and energy equations have been worked out using locally one-dimensional difference scheme of A.A. Samarskii, where the central differences have been used for diffusive terms and difference scheme with donor cells are used for the convective terms. The corresponding system of linear equations has been worked out by the Thomas method. An in-house computational code has been developed using the C++ programming language. More detailed description and flowchart can be found in previous published papers (Mikhailenko *et al.*, 2018; Mikhailenko and Sheremet, 2020; Mikhailenko *et al.*, 2020).

The developed mathematical model and computational code have been tested for compliance by solving selected tasks. The rotating model has been verified by the challenge of thermal convective transport in a differentially heated chamber. Figure 2 illustrates a good comparison of the obtained data with experimental results of Hamady *et al.* (1994) and computational results of Tso *et al.* (2007). The results have been obtained for $Ra = 3 \times 10^5$, $Pr = 0.7$ and different rotation angles.

The variable heating model has been tested by solving the problem of thermogravitational natural convection in a chamber with time-dependent temperature on the heated border. Figure 3 demonstrates a nice concordance between the obtained isolines and data of Kazmierczak and Chinoda (1992). The data have been received for $Ra = 1.4 \times 10^5$, $Pr = 7$ and $\tau = 0.035$.

Analysis of mesh sensitivity has been demonstrated in Figure 4. Three various grids of 60×60, 120×120 and 240×240 elements have been used. It can be observed that data do not have essential differences between the second and third grids. Therefore, a uniform grid of 120×120 elements has been chosen for further research.

4. Results and discussion

The calculations are performed for the following magnitudes of the determining characteristics: the Rayleigh number ($Ra = 10^5$), the Prandtl number ($Pr = 0.7$), the Taylor number ($Ta = 10^3 - 10^6$), surface emissivity ($\varepsilon = 0.0 - 0.9$) and the volumetric thermal generation frequency ($f = 0.1$ and $f = 0.01$). It should be noted that material of the local heater is silicon, the material of bottom wall is textolite and the material of other walls is aluminum. Therefore, the considered thermal conductivity ratio and thermal diffusivity ratio are $\lambda_{hs}/\lambda_f = 5714.29$, $\lambda_w/\lambda_f = 7857.14$ (for aluminum walls), $\lambda_w/\lambda_f = 14.2857$ (for

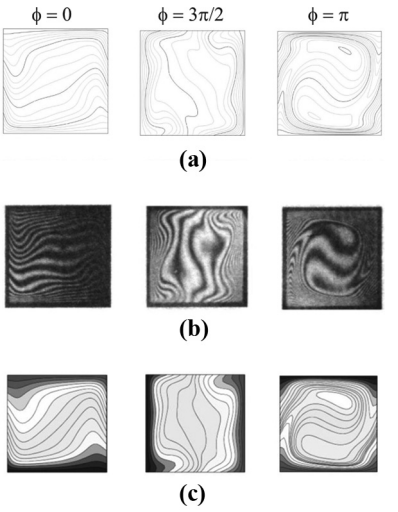

Figure 2.
Comparison of isotherms for various rotation angles at $Ra = 3 \times 10^5$ and $Pr = 0.7$

Notes: (a) Obtained results; (b) experimental data of Hamady *et al.* (1994); (c) numerical results of Tso *et al.* (2007)

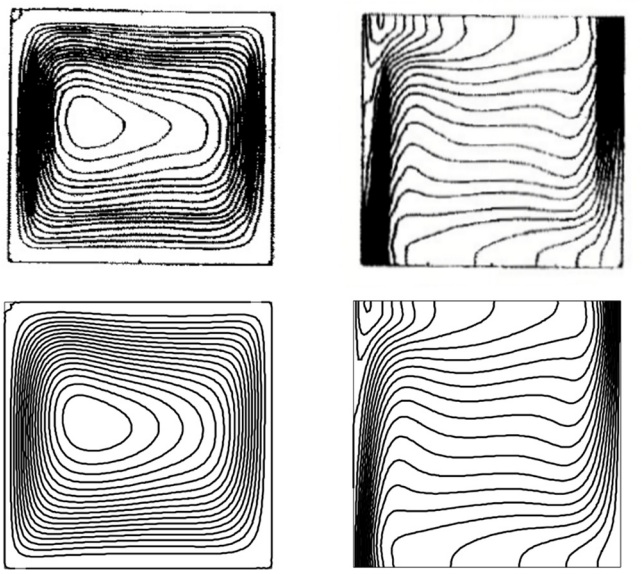

Figure 3.
Comparison of isolines at $Ra = 1.4 \times 10^5$, $Pr = 7$ and $\tau = 0.035$ with results (Kazmierczak and Chinoda, 1992)

textolite wall), $\alpha_{hs}/\alpha_f = 4.15888$, $\alpha_w/\alpha_f = 3.8785$ (for aluminum wall) and $\alpha_w/\alpha_f = 0.0116822$ (for textolite wall). The streamlines and isotherms for different rotation angles during one complete revolution of the chamber have been obtained and described in detail. There are many cavity revolutions during one period of heating because it is greater than rotation

period. Fluid circulation structure and the temperature patterns are different slightly for adjacent revolutions and repeating every heating period. The fluid circulation strength, mean temperature within the heat source, mean convective and radiative *Nu* have been used for describing the effect of angular velocity, time-dependent volumetric heating frequency and surface emissivity.

Figure 5 demonstrates streamlines for one complete revolution at $Ta = 10^4$, $\varepsilon = 0.9$ and $f = 0.01$. A complex flow with the formation and development of new convective cells is defined by the considered physical formulation of the problem and the values of key parameters. So, at the angle of rotation $\phi = 0$, one can observe a large vortex occupying the main space, the motion in which occurs in a clockwise direction. A small vortex with counterclockwise medium circulation can be observed to the left of the heat-conducting block. A small vortex develops and begins to dominate the initially larger circulation in the process of rotation during $0 < \phi < \pi/2$. This is manifested in the weakening of this previously main vortex and reforming it into several smaller recirculation structures. Such a restructuring of the flow strongly affects the intensity of convective flows. At $\phi = 3\pi/4$, one

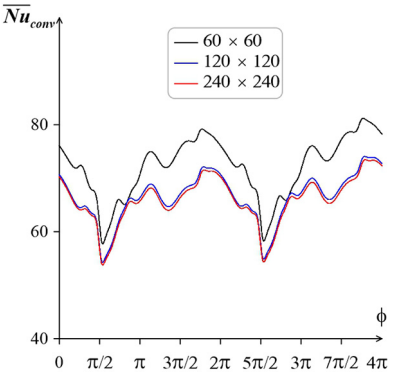

Figure 4.
Evolution of mean convective *Nu* during two cavity revolutions at $Ta = 10^4$, $\varepsilon = 0.3$, $f = 0.1$ and different meshes

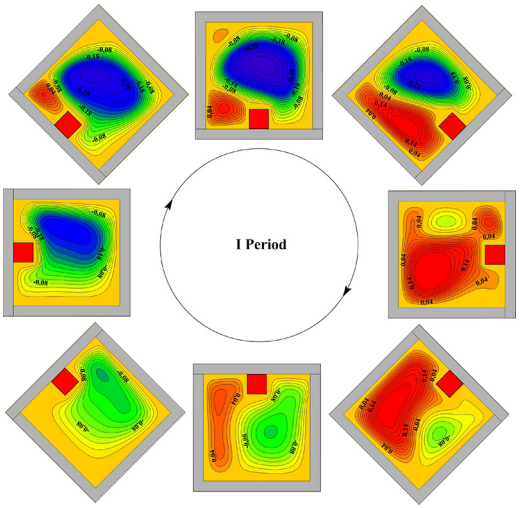

Figure 5.
Isolines of stream function for full revolution at $Ta = 10^4$, $\varepsilon = 0.9$ and $f = 0.01$

large vortex is observed in the cavity, but for this time, the fluid moves in a counterclockwise direction. At the same time, another convective cell with clockwise circulation appears and starts to grow to the left of the source. A new vortex evolving during rotation up to $\phi = 3\pi/2$. While at $\phi = 7\pi/4$, a new circulation counterclockwise arises at left down corner of chamber. Thus, the complete revolution of the cavity can be described as two successive processes of the formation and development of convective cells, with the fluid flow in the counterclockwise direction in the first case and clockwise in the second.

Figure 6 demonstrates isotherms during one complete revolution for $Ta = 10^4$, $\varepsilon = 0.9$ and $f = 0.01$. It must be emphasized that the thermal conductivity of the bottom wall differs from the heat conductivity of other solid walls and corresponds to the textolite, while others correspond to aluminum. Therefore, the temperature on the lower heat-conducting wall is distributed from the central heater area to the sides. While other walls are well cooled from the external vertical boundaries and have a low temperature.

At $\phi = 0$, one can observe a thermal plume emanating from a source of energy and shifting to the left side, while the most volume is occupied by the circulating cold medium. The thermal plume begins to rise because of the influence of buoyancy force during the cavity rotation at $0 < \phi < \pi/2$. At the same time, cold fluid flows within the free space have an essential influence on this process. At $\phi = \pi/2$, the cavity, as well as the heat source and the plume, have the counterclockwise motion, while fluid circulates in the opposite direction. This leads to the previously described complex restructuring of the flow. The plume core reorients in vertical direction during rotation at $\pi/2 < \phi < \pi$. Further, in the process of rotation at $3\pi/2 < \phi < 2\pi$, the thermal plume adjoins to the left wall. The direction of flow within the chamber is defined by the circulation of a cold medium. At this time, the convective heat transfer is intensified.

Figure 7 demonstrates the effect of the surface emissivity on mean convective and radiative *Nu*, fluid circulation strength and average heat source temperature.

The demonstrated two revolutions correspond to the moment when the heat generation in the source reaches maximum. The magnitudes of the studied characteristics differ slightly in two adjacent cavity revolutions. An interesting fact is that the decrease in the heat flux of the heating source begins after 2π, but the values of the parameters are grown.

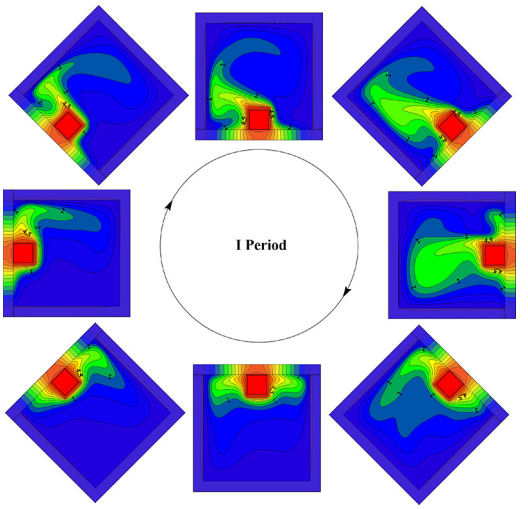

Figure 6.
Isolines of temperature for full revolution at $Ta = 10^4$, $\varepsilon = 0.9$ and $f = 0.01$

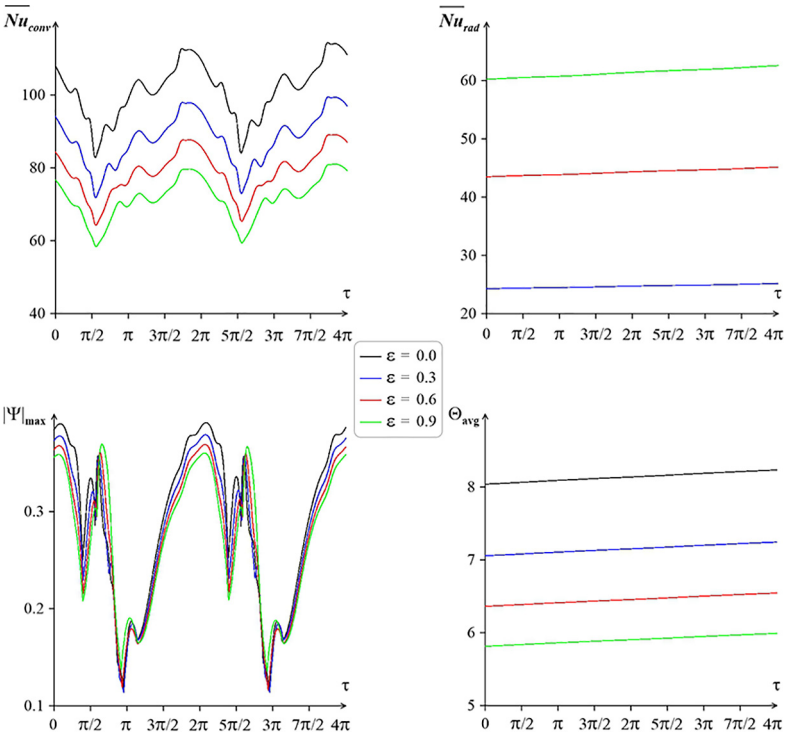

Figure 7.
Variations of mean convective and radiative *Nu*, fluid motion strength and mean temperature within the heat source for two complete revolutions at $Ta = 10^4$, $f = 0.01$ and different ε

This effect can be observed in detail in figures presented for the full heating period. Increasing surface emissivity reduces convective heat transfer. The radiative *Nu* increases. A rise of ε results in a slight diminution of the flow intensity, but the average temperature within the heat source decreases because of an increase in the total energy transport. One can see a sharp decrease in the intensity of the fluid flow, which is associated with a sharp restructuring of the flow during the rotation of the cavity between the angles $\phi = 0$ and $\phi = \pi/2$ (see Figure 5). An even more intense restructuring of the flow is associated with a decrease in $|\Psi|_{\max}$ to the angle of rotation $\phi = \pi$. With further rotation, the value increases, because the cavity is occupied by one dominant convective cell. The decrease in Nu_{conv} at the angle of rotation $\phi = \pi/2$ is associated with the circulation of the thermal plume (see Figure 6) around the heater. At this moment, the temperature difference between the solid block and the surrounding air takes on a minimum value.

It should be noted that an analysis of the convective heat transfer and thermal radiation within a diathermal medium is more essential in the case of solid wall chambers. Such opinion can be explained by the surface radiation effect only from the adiabatic walls or walls of finite thickness. The latter can be explained by the indirect influence of thermal radiation on heat transfer in a cavity, namely, initially thermal radiation changes the temperature field within the solid walls and after that because of solid wall heat conduction one can find an influence of wall heat conduction on convective heat transfer within the cavity.

Figure 8 illustrates the impacts of the angular velocity and surface emissivity on the liquid circulation strength, complex heat transfer, as well as the average temperature within

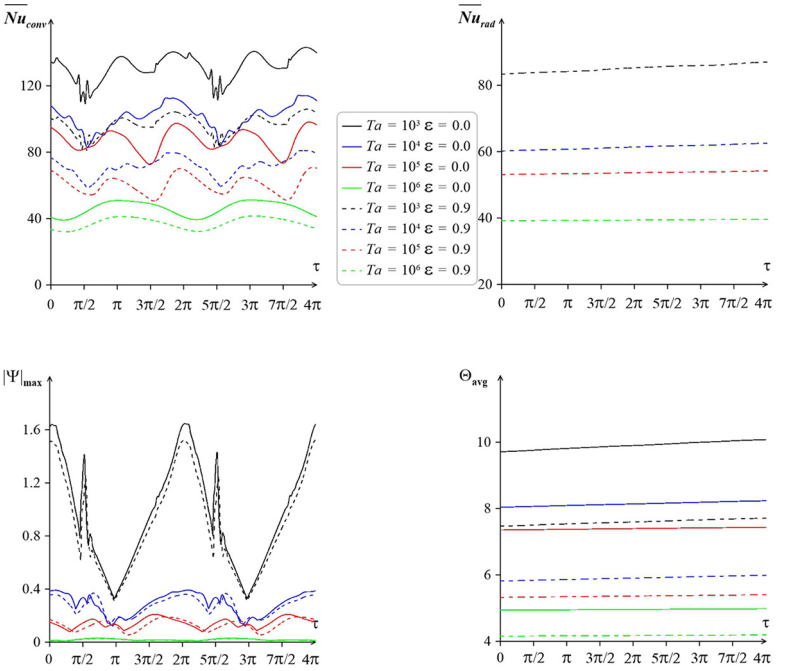

Figure 8.
Variations of mean average *Nu*, fluid circulation strength and mean temperature inside the heat source during two complete revolutions for $f = 0.01$ and ε and *Ta*

a heat source for two full revolutions. The intensity of the flow decreases in the first half of the revolution, when the direction of movement of the heating block is opposite to the meeting flows, while it grows in the second half of the revolution, when the direction of movement of the block coincides with the direction of fluid flow. It is interesting to highlight that $|\Psi|_{\max}$ and convective Nusselt number are subject to rotation effect, while the radiation *Nu* and mean temperature inside the element practically do not change during the revolution of the cavity. The change in radiation *Nu* and mean temperature is because of unsteady heat generation in the solid block, the period of which is greater than the rotation period. A rise of the angular velocity of the cavity results in a reduction of the intensity of the liquid motion and convective energy transport. Also, a decrease in the average radiation *Nu* and the mean temperature inside the energy-generated element is found with a growth of the Taylor number. It seems that the latter is owing to the thermal conduction in solid walls. A diminution of the average temperature within the source with a rising of ε is observed as before. Moreover, this effect is weakened with an increase in the Taylor number.

Figure 9 presents the effects of ε and f on liquid circulation strength, mean average convection and radiation *Nu* and mean temperature inside the heater for $Ta = 10^4$ during periods of heating. The investigated parameters are shown for one heating period at $f = 0.01$ and for ten periods at $f = 0.1$. As noted earlier, the results show lower parameters values with increasing of ε. Consider the case of $f = 0.01$. The start ($\tau = 3{,}927$) and the end ($\tau = 4{,}555$) of time correspond to the minimum heat flux in the heated source, and $\tau = 4{,}241$ corresponds to the maximum value. The studied values, for example, average convective Nusselt number has local minimum and maximum at other points, which indicates a small delay in parameter changes. In the case of $f = 0.1$, the oscillation amplitude of the studied characteristics

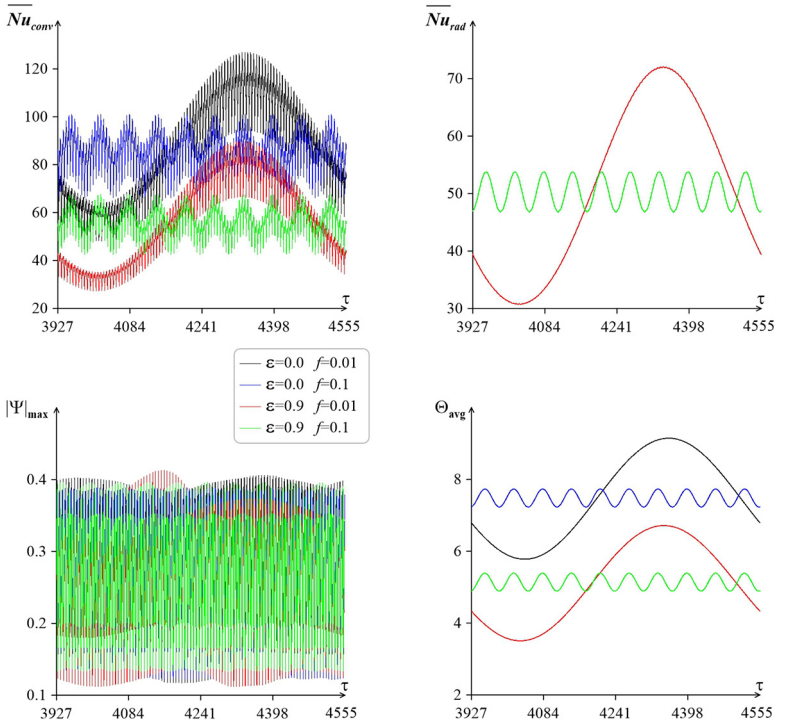

Figure 9. Variations of mean *Nu*, fluid circulation strength and mean temperature inside the heat source during heating period for $Ta = 10^4$ and different ε and f

decreases. Time-averaged values of *Nu* and the average temperature within the source during one heating period are practically equal in both cases and can be seen in Table 1.

Figure 10 shows impacts of Taylor number and f on liquid circulation strength, mean convection and radiation *Nu* and mean temperature inside a heater for $\varepsilon = 0.9$ during periods of heating. The previously described patterns of changing the heating frequency are kept for the same values of the Taylor number.

Figures clearly show that convective Nusselt and the intensity of the flow are changed because of the influence of unsteady heating and rotation, while radiation *Nu* and mean temperature inside the heater are changed because of unsteady heating only. This suggests that the mechanisms of heating and thermal radiation suppress the effect of rotation. A rise of the Taylor number results in a decrease in the average temperature within the source and not in all cases. For example, the local minimum of θ_{avg} in the case of $Ta = 10^3$ and $f = 0.01$ is lower compared to the case of $Ta = 10^6$ and different f. But the average temperature within the source during one heating period decreases with Ta and it can be seen in Table 2. Also, an interesting fact is that an influence of the heating frequency decreases with a growth of the Taylor number.

Table 1. Time averaged values of Nu_{conv} and θ_{avg} during heating period for $Ta = 10^4$ and different ε and f

Parameters	Nu_{conv}	θ_{avg}
$\varepsilon = 0.0$ and $f = 0.01$	86.2231	7.46199
$\varepsilon = 0.0$ and $f = 0.1$	86.0422	7.48071
$\varepsilon = 0.9$ and $f = 0.01$	56.2928	5.11202
$\varepsilon = 0.9$ and $f = 0.1$	56.3418	5.1397

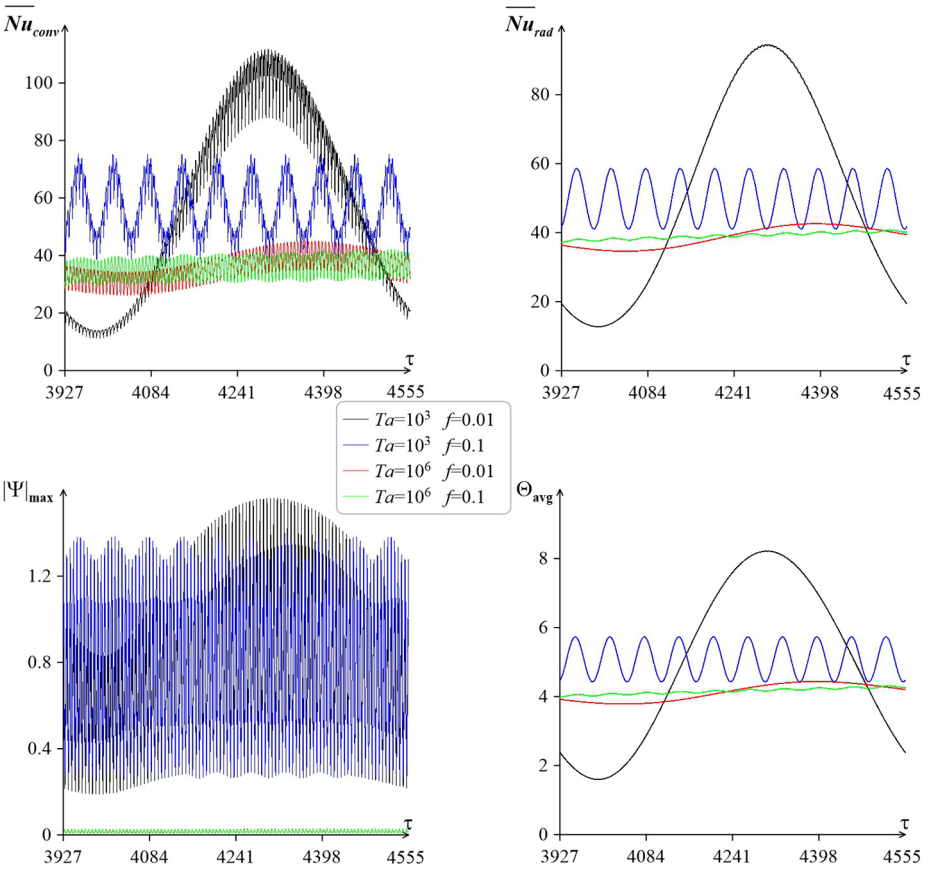

Figure 10.
Variations of mean convection and radiation *Nu*, circulation intensity and mean temperature inside the heat source during heating period for $\varepsilon = 0.9$ and different *Ta* and *f*

Table 2.
Time averaged θ_{avg} during heating period for $\varepsilon = 0.9$ and different *Ta* and *f*

Parameters	θ_{avg}
$Ta = 10^3$ and $f = 0.01$	4.94534
$Ta = 10^3$ and $f = 0.1$	5.078
$Ta = 10^6$ and $f = 0.01$	4.11708
$Ta = 10^6$ and $f = 0.1$	4.15767

Figure 11 presents the changes of the liquid circulation strength, convective and radiative rate of heat transfer, as well as the average temperature within a heat source for $\varepsilon = 0.9$ during two full revolutions of the cavity. As shown earlier, parameters can take different values at different rotations of the cavity during the heating period. This is more significant at low Taylor numbers. The obtained results correspond to the moment when the thermal flux within the source reaches the highest magnitude. An unsteady heat flux in the source simulates the heating of an electronic equipment element because of the electric currents passing in it. The electronic chip may be defenseless to temperatures at maximum load; therefore, such results may be interested in practice. The $|\Psi|_{max}$ value decreases with increasing of the Taylor

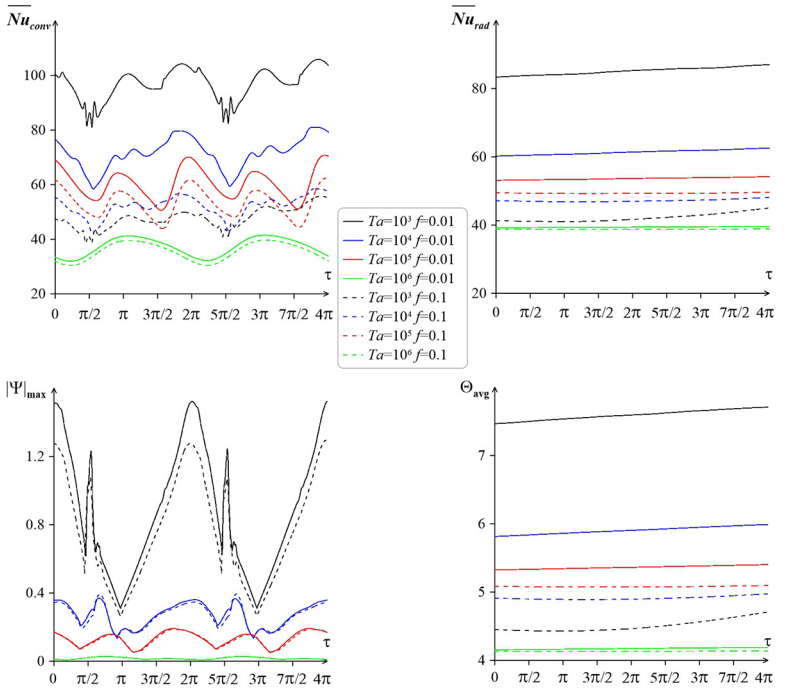

Figure 11.
Variations of mean convection and radiation Nu, circulation strength and mean temperature inside the heat source during two full revolutions for $\varepsilon = 0.9$ and different Ta and f

number. With an increase in the Taylor number, a decrease in convective Nusselt number is observed in the case of $f = 0.01$. An increase in the Taylor number leads to an increase in the intensity of the heat transfer in the case of $f = 0.1$, except for $Ta = 10^6$. The same can be observed in changes of the average radiation Nusselt number. Low values of angular velocity and long heating period lead to high average temperatures within the source. The lowest temperature is reached at high Taylor values or high heating frequencies.

5. Conclusions

Complex energy transport in a rotating chamber having variable thermally generated element and solid walls has been scrutinized computationally. The control equations have been written using stream function, vorticity and temperature. The set of differential equations has been discretized and worked out using the finite difference technique on a uniform grid. The effects of surface emissivity, angular velocity and volumetric thermal generation frequency have been discussed using the motion strength, mean temperature within the heat source, convective and radiative average Nusselt numbers. Also, isotherms and streamlines have been shown and described in detail. Main conclusions are as follows:

- A rise of surface emissivity leads to diminution of the mean temperature inside the heater.
- A rise of volumetric thermally generated frequency results in a decrease of oscillation amplitude. In the same time, the average parameters values during one heating period are changed insignificantly.

- A weak rotation can improve the heat transfer in the case of $f = 0.1$. The average heater temperature during full period of heat generation reduces with Ta.
- At the moment when the thermal flux within the source has the highest value, better heat transfer has been observed in the case of low values of both angular velocity and volumetric heat generation frequency.

References

Abdollahzadeh Jamalabadi, M.Y., Ghassemi, M. and Hamedi, M.H. (2013), "Numerical investigation of thermal radiation effects on open cavity with discrete heat sources", *International Journal of Numerical Methods for Heat and Fluid Flow*, Vol. 23 No. 4, pp. 649-661, doi: 10.1108/09615531311323791.

Alsabery, A.I., Mohebbi, R., Chamkha, A.J. and Hashim, I. (2019), "Effect of local thermal non-equilibrium model on natural convection in a nanofluid-filled wavy-walled porous cavity containing inner solid cylinder", *Chemical Engineering Science*, Vol. 201, pp. 247-263, doi: 10.1016/j.ces.2019.03.006.

Alsabery, A.I., Siddheshwar, P.G., Saleh, H. and Hashim, I. (2016), "Transient free convective heat transfer in nanoliquid-saturated porous square cavity with a concentric solid insert and sinusoidal boundary condition", *Superlattices and Microstructures*, Vol. 100, pp. 1006-1028, doi: 10.1016/j.spmi.2016.10.062.

Alsabery, A.I., Tayebi, T., Chamkha, A.J. and Hashim, I. (2018), "Effect of rotating solid cylinder on entropy generation and convective heat transfer in a wavy porous cavity heated from below", *International Communications in Heat and Mass Transfer*, Vol. 95, pp. 197-209, doi: 10.1016/j.icheatmasstransfer.2018.05.003.

Alsabery, A.I., Chamkha, A.J., Saleh, H., Hashim, I. and Chanane, B. (2017), "Effects of finite wall thickness and sinusoidal heating on convection in nanofluid-saturated local thermal non-equilibrium porous cavity", *Physica A: Statistical Mechanics and Its Applications* , Vol. 470, pp. 20-38, doi: 10.1016/j.physa.2016.11.107.

Ayachi, R.E., Raji, A., Hasnaoui, M., Naïmi, M. and Abdelbaki, A. (2012), "Combined effects of radiation and natural convection in a square cavity submitted to two combined modes of cross gradients of temperature", *Numerical Heat Transfer, Part A: Applications*, Vol. 62 No. 11, pp. 905-931, doi: 10.1080/10407782.2012.712463.

Bahlaoui, A., Raji, A. and Hasnaoui, M. (2006), "Combined effect of radiation and natural convection in a rectangular enclosure discreetly heated from one side", *International Journal of Numerical Methods for Heat and Fluid Flow*, Vol. 16 No. 4, pp. 431-450, doi: 10.1108/09615530610653073.

Banerjee, S., Mukhopadhyay, A., Sen, S. and Ganguly, R. (2009), "Thermomagnetic convection in square and shallow enclosures for electronics cooling", *Numerical Heat Transfer, Part A: Applications*, Vol. 55 No. 10, pp. 931-951, doi: 10.1080/10407780902925440.

Billaud, Y., Saury, D. and Lemonnier, D. (2017), "Numerical investigation of coupled natural convection and radiation in a differentially heated cubic cavity filled with humid air. Effects of the cavity size", *Numerical Heat Transfer, Part A: Applications*, Vol. 72 No. 7, pp. 495-518, doi: 10.1080/10407782.2017.1386509.

Boukendil, M., El Moutaouakil, L., Zrikem, Z. and Abdelbaki, A. (2020), "Coupled thermal radiation and natural convection heat transfer in a cavity with a discretely heated inner body", *Materials Today: Proceedings*, Vol. 27, doi: 10.1016/j.matpr.2020.03.548.

El Ayachi, R., Raji, A., Hasnaoui, M. and Bahlaoui, A. (2008), "Combined effect of radiation and natural convection in a square cavity differentially heated with a periodic temperature", *Numeric Heat Transfer, Part A: Applications*, Vol. 53 No. 12, pp. 1339-1356, doi: 10.1080/10407780801960043.

Fedyushkin, A.I. (2019), "Heat and mass transfer during crystal growing by the Czochralski method with a submerged vibrator", *Journal of Physics: Conference Series*, Vol. 1359, doi: 10.1088/1742-6596/1359/1/012054.

Ghasemi, B. (2005), "Mixed convection in a rectangular cavity with a pulsating heated electronic component", *Numerical Heat Transfer, Part A: Applications*, Vol. 47 No. 5, pp. 505-521, doi: 10.1080/10407780590886278.

Hamady, F.J., Lloyd, J.R., Yang, K.T. and Yang, H.Q. (1994), "A study of natural convection in a rotating enclosure", *Journal of Heat Transfer*, Vol. 116 No. 1, pp. 136-143, doi: 10.1115/1.2910847.

Huang, Z., Zhang, W. and Xi, G. (2014), "Natural convection heat transfer in a cubic cavity submitted to time-periodic sidewall temperature", *Numerical Heat Transfer, Part A: Applications*, Vol. 67 No. 1, pp. 13-32, doi: 10.1080/10407782.2013.798550.

Jena, S.K. and Mahapatra, S.K. (2014), "A numerical investigation of surface radiation interaction with magneto-convection of an electrically conducting fluid imposed with a transverse magnetic field", *Heat Transfer Engineering*, Vol. 36 No. 1, pp. 21-32, doi: 10.1080/01457632.2014.897584.

Jin, L.F., Tou, K.W. and Tso, C.P. (2005), "Experimental and numerical studies in a rotating cavity with discrete heat sources with conjugate effects", *Experimental Heat Transfer* , Vol. 18 No. 4, p. 259, doi: 10.1080/08916150500201552.

Kazmierczak, M. and Chinoda, Z. (1992), "Buoyancy-driven flow in an enclosure with time periodic boundary conditions", *International Journal of Heat and Mass Transfer*, Vol. 35 No. 6, pp. 1507-1518, doi: 10.1016/0017-9310(92)90040-Y.

Kogawa, T., Shoji, E., Okajima, J., Komiya, A. and Maruyama, S. (2019), "Experimental evaluation of thermal radiation effects on natural convection with a Rayleigh number of 10^8–10^9 by using an interferometer", *International Journal of Heat and Mass Transfer*, Vol. 132, pp. 1239-1249, doi: 10.1016/j.ijheatmasstransfer.2018.11.162.

Mikhailenko, S.A. and Sheremet, M.A. (2020), "Impacts of rotation and local element of variable heat generation on convective heat transfer in a partially porous cavity using local thermal non-equilibrium model", *International Journal of Thermal Sciences*, Vol. 155, p. 106427, doi: 10.1016/j.ijthermalsci.2020.106427.

Mikhailenko, S.A., Sheremet, M.A. and Mohamad, A.A. (2018), "Convective-radiative heat transfer in a rotating square cavity with a local heat-generating source", *International Journal of Mechanical Sciences*, Vol. 142-143, pp. 530-540, doi: 10.1016/j.ijmecsci.2018.05.030.

Mikhailenko, S.A., Sheremet, M.A. and Pop, I. (2020), "Natural convection combined with surface radiation in a rotating cavity with an element of variable volumetric heat generation", *Energy*, Vol. 210, pp. 118543, doi: 10.1016/j.energy.2020.118543.

Miroshnichenko, I.V., Sheremet, M.A. and Mohamad, A.A. (2016), "Numerical simulation of a conjugate turbulent natural convection combined with surface thermal radiation in an enclosure with a heat source", *International Journal of Thermal Sciences*, Vol. 109, pp. 172-181, doi: 10.1016/j.ijthermalsci.2016.06.008.

Nguyen, T.H.T., Chen, J.C., Hu, C. and Chen, C.H. (2019), "Numerical simulation of heat and mass transfer during Czochralski silicon crystal growth under the application of crystal-crucible counter- and iso-rotations", *Journal of Crystal Growth*, Vol. 507, pp. 50-57, doi: 10.1016/j.jcrysgro.2018.10.049.

Nouanegue, H.F., Muftuoglu, A. and Bilgen, E. (2009), "Heat transfer by natural convection, conduction and radiation in an inclined square enclosure bounded with a solid wall", *International Journal of Thermal Sciences*, Vol. 48 No. 5, pp. 871-880, doi: 10.1016/j.ijthermalsci.2008.06.008.

Oosthuizen, P.H. (1999), "Unsteady free convective flow in an enclosure with a stepwise periodically varying side-wall heat flux", *International Journal of Numerical Methods for Heat and Fluid Flow*, Vol. 9 No. 3, pp. 214-223, doi: 10.1108/09615539910260095.

Ridouane, E.H., Hasnaoui, M., Amahmid, A. and Raji, A. (2004), "Interaction between natural convection and radiation in a square cavity heated from below", *Numerical Heat Transfer, Part A: Applications*, Vol. 45 No. 3, pp. 289-311, doi: 10.1080/10407780490250373.

Saravanan, S. and Sivaraj, C. (2017), "Combined thermal radiation and natural convection in a cavity containing a discrete heater: effects of nature of heating and heater aspect ratio", *International Journal of Heat and Fluid Flow*, Vol. 66, pp. 70-82, doi: 10.1016/j.ijheatfluidflow.2017.05.004.

Sedelnikov, G.A., Busse, F.H. and Lyubimov, D.V. (2012), "Convection in a rotating cubical cavity", *European Journal of Mechanics – B/Fluids*, Vol. 31, pp. 149-157, doi: 10.1016/j.euromechflu.2011.06.001.

Sen, S. and Sarkar, A. (1995), "Effects of variable property and surface radiation on laminar natural convection in a square enclosure", *International Journal of Numerical Methods for Heat and Fluid Flow*, Vol. 5 No. 7, pp. 615-627, doi: 10.1108/EUM0000000004080.

Sheremet, M.A., Pop, I. and Mahian, O. (2018), "Natural convection in an inclined cavity with time-periodic temperature boundary conditions using nanofluids: application in solar collectors", *International Journal of Heat and Mass Transfer*, Vol. 116, pp. 751-761, doi: 10.1016/j.ijheatmasstransfer.2017.09.070.

Sivaraj, C. and Sheremet, M.A. (2018), "Convective–radiative heat transfer in a cavity filled with a nanofluid under the effect of a nonuniformly heated plate", *International Journal of Numerical Methods for Heat and Fluid Flow*, Vol. 28 No. 6, pp. 1392-1409, doi: 10.1108/HFF-06-2017-0255.

Sivasankaran, S., Alsabery, A.I. and Hashim, I. (2018), "Internal heat generation effect on transient natural convection in a nanofluid-saturated local thermal non-equilibrium porous inclined cavity", *Physica A: Statistical Mechanics and Its Applications*, Vol. 509, pp. 275-293, doi: 10.1016/j.physa.2018.06.036.

Tso, C.P., Jin, L.F. and Tou, K.W. (2007), "Numerical segregation of the effects of body forces in a rotating, differentially heated enclosure", *Numerical Heat Transfer, Part A: Applications*, Vol. 51 No. 1, pp. 85-107, doi: 10.1080/10407780600710318.

Wang, Z., Yang, M., Li, L. and Zhang, Y. (2011), "Combined heat transfer by natural convection – conduction and surface radiation in an open cavity under constant heat flux heating", *Numerical Heat Transfer, Part A: Aplications*, Vol. 60 No. 4, pp. 289-304, doi: 10.1080/10407782.2011.594415.

Wu, W., Amsbeck, L., Buck, R., Waibel, N., Langner, P. and Pitz-Paal, R. (2014), "On the influence of rotation on thermal convection in a rotating cavity for solar receiver applications", *Applied Thermal Engineering*, Vol. 70 No. 1, pp. 694-704, doi: 10.1016/j.applthermaleng.2014.03.059.

Xin, S., Salat, J., Joubert, P., Sergent, A., Penot, F. and Quéré, P.L. (2013), "Resolving the stratification discrepancy of turbulent natural convection in differentially heated air-filled cavities. Part III: a full convection–conduction–surface radiation coupling", *International Journal of Heat and Fluid Flow*, Vol. 42, pp. 33-48, doi: 10.1016/j.ijheatfluidflow.2013.01.021.

Zargartalebi, H., Ghalambaz, M., Khanafer, K. and Pop, I. (2017), "Unsteady conjugate natural in a porous cavity boarded by two vertical finite thickness walls", *International Communications in Heat and Mass Transfer*, Vol. 81, pp. 218-228, doi: 10.1016/j.icheatmasstransfer.2016.12.016.

Zhang, W., Zhang, C. and Xi, G. (2011), "Conjugate conduction-natural convection in an enclosure with time-periodic sidewall temperature and inclination", *International Journal of Heat and Fluid Flow*, Vol. 32 No. 1, pp. 52-64, doi: 10.1016/j.ijheatfluidflow.2010.08.006.

Zhang, W., Huang, Z., Zhang, C. and Xi, G. (2012), "Conjugate wall conduction-fluid natural convection in a three-dimensional inclined enclosure", *Numerical Heat Transfer, Part A: Applications*, Vol. 61 No. 2, pp. 122-141, doi: 10.1080/10407782.2012.638509.

Corresponding author
Mikhail A. Sheremet can be contacted at: michael-sher@ya.ru